

7. G. I. Maikapar, "Separated flows on the leeward side of a delta wing and a solid of revolution in a supersonic flow," Uch. Zap. Tsentr. Aerogidrod. Inst., 18, No. 4 (1982)
8. L. G. Vasenev and A. M. Kharitonov, "Interference of a delta wing and a cylindrical body at supersonic velocity," Preprint, Inst. Teor. Prikl. Mekh. Sib. Otd. Akad. Nauk SSSR, Novosibirsk, No. 28-84 (1984).
9. K. Y. Narayan, "Leeside flowfield and heat transfer of a delta wing at $M_\infty = 10$," AIAA J., 16, No. 2 (1978).
10. A. K. Rastogi and W. Rodi, "Calculation of general three-dimensional turbulent boundary layers," AIAA J., 16, No. 2 (1978).
11. S. I. Shpak, "Calculation of a triangular incompressible turbulent boundary layer," Preprint, Inst. Teor. Prikl. Mekh. Sib. Otd. Akad. Nauk SSSR, No. 35-81 (1981),
12. B. M. Bulakh, Nonlinear Conical Gas Flows [in Russian], Nauka, Moscow (1970).
13. G. P. Voskresenskii, A. S. Il'ina, and V. S. Tatarenchik, "Supersonic flow about wings with an attached shock wave," Tr. TsAGI, No. 1590 (1974).
14. W. J. Bannik and C. Nebbeling, "An experimental investigation of the expansion flow field over a delta wing at supersonic speed," Rept/Delft Univ. Technol., VTH-167, Netherlands (1971).
15. K. C. Wang, "On the determination of zones of influence and dependence for three-dimensional boundary-layer equations," J. Fluid Mech., 48, No. 2 (1971).
16. B. Roux and B. Forestier, "Analysis of a compressible laminar boundary layer on a yawed cone," AIAA J., 14, No. 8 (1976).
17. G. N. Dudin, "Finite-difference method of solving three-dimensional boundary-layer equations for the regime of strong viscous interaction," Tr. Tsentr. Aerogidrod. Inst., No. 2190 (1983).

SUPERSONIC FLOW OVER DELTA WINGS AND
ELEMENTS OF STAR-SHAPED BODIES AT
ANGLES OF ATTACK AND ROLL

O. N. Ivanov and A. I. Shvets

UDC 533.6.011.55+629.782.015.3

Since the sixties there has been widespread investigation of the flow over triangular delta wings (e.g., [1-3]). It has been shown theoretically and experimentally that at supersonic speed a delta wing has a larger L/D than an equivalent planar triangular wing. In addition to studies of flow over lifting surfaces the aerodynamic characteristics of star shapes have been investigated [4-6]. These shapes, whose elements can be considered as delta wings, have considerably less drag at supersonic speeds than equivalent axisymmetric bodies.

In flight conditions one can achieve a flow regime where the plane of the angle of attack does not coincide with the plane of symmetry of a star-shaped body. Asymmetrical flow over delta wings forms in some cases at angles of attack and roll and also where there is asymmetry of the original wing shape. There are very few papers dealing with asymmetric flow over delta wings. Possible asymmetric shock wave patterns on delta wings have been studied [7]; in investigations of slip flow over delta wings of vertex angle $\Lambda > 150^\circ$ calculations of the pressure distribution and the aerodynamic characteristics have been combined with direct measurements of pressure, force and momentum at $M = 7.8-15.5$ [8].

This paper gives results of experiments on supersonic flow over delta wings at angles of attack and roll. In contrast with [8] we studied the flow over delta wings over a wide range of vertex angle (Λ is the angle between the wetted surfaces of the delta wing) with both a curved shock wave, and with a shock system positioned between the wings, corresponding to Mach and regular interaction. At large vertex angles ($\Lambda = 150-180^\circ$) the flow systems studied show flow asymmetry of a vehicle with delta wings, and for values of vertex angle ($\Lambda < 90$) they show flow over an element of a star-shaped body.

1. Experimental Technique and Model Description. Tests were made in a short-duration wind tunnel of the Institute of Mechanics, MGU. The aerodynamic facility has a closed

Moscow. Translated from Zhurnal Prikladnoi Mekhaniki i Tekhnicheskoi Fiziki, No. 1, pp. 81-87, January-February, 1989. Original article submitted November 9, 1987.

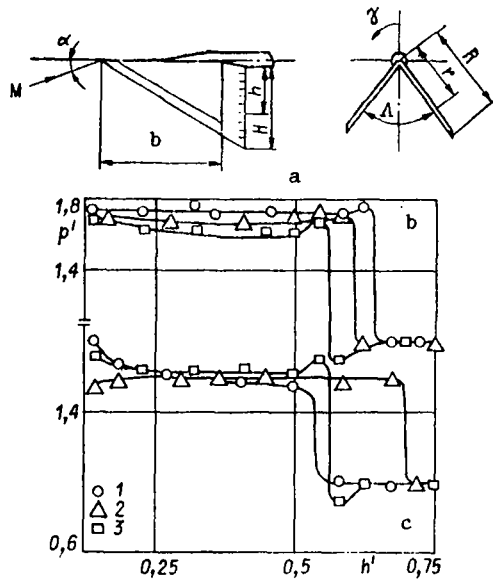


Fig. 1

working section of dimensions 600×600 mm and an adjustable diffuser. The nonuniformity of the flow field in the vicinity of the model location was 1%. The Mach number of the unperturbed incident stream is $M = 3$, and the Reynolds number computed from the incident flow parameters, and based on 0.1 m, is $Re = 3 \cdot 10^6$. The test program for the delta wing was conducted at angles of attack of $\alpha = 0, 5, 10, 15^\circ$, vertex angles of $\Lambda = 180, 150, 120, 90, 60^\circ$, and roll angles of $\gamma = 0, 20, 40, 60^\circ$.

The model surface pressure was measured using a type DMI-0.1 inductive sensor mounted in a pressure switch device. The relative rms measurement error of the pressure coefficient was $\sigma_{c_p} = 0.02$.

For the tests on pressure distribution in asymmetric flow over a delta wing a structure was prepared in which one could vary Λ and γ relative to the line of intersection of the internal surfaces of the wings (the mean chord) in a body-fixed coordinate system (Fig. 1, a). The sweepback angle in the wing plane was $\chi = 60^\circ$. The model was supported at its base by a clamp of diameter 25 mm, fastened in a saber-shaped suspension. The length (mean chord) of the delta wing test model was $b = 238$ mm, the semi-dimension along the trailing edge at $\Lambda = 180^\circ$ was $R = 138$ mm, and the thickness of the delta wing arm was 12 mm. The leading edges of the wings had a wedge-shaped taper towards the shaded side with an angle of 15° . The model surface had 18 pressure tap orifices at a pitch of 6 mm in a section located at distance 30 mm from the trailing edge of the wing.

2. The Delta Wing. At a certain distance behind the model in the region bounded by the characteristics issuing from the trailing edge of the wing the flow remains similar to that inside the wings. Therefore by measuring the total pressures at some distance from the trailing edge with the aid of a Pitot tube rake one can evaluate the total pressure inside the deflection of the delta wings. The total pressure was expressed in the form of the dependence $p' = f(h')$, where $p' = p'_0/p'_\infty$, $h' = h/H$, p'_0 is the total pressure measured by the Pitot tube, h is the distance from the line of intersection of the inner surfaces of the wings to the Pitot tube, and H is the distance in the section of the rake to the plane of the leading edge of the wing (Fig. 1, a).

In symmetric flow the total pressure in the plane of symmetry of the wings varies discontinuously, taking on different constant values in different sections. The first low pressure section corresponds to the region of unperturbed flow, and the second section, one of increased pressure, is formed as a result of the pressure increase behind the shock. With increase of γ (Fig. 1, b: $\Lambda = 90^\circ$; $\alpha = 15^\circ$; 1-3) $\gamma = 0, 20, 40^\circ$) the second section of increased pressure diminishes, the pressure discontinuity moves closer to the model axis, and with a decrease of Λ (Fig. 1, c: $\alpha = 15^\circ$; $\gamma = 40^\circ$; 1-3) $\Lambda = 120, 90, 60^\circ$) the pressure in the second section remains almost unchanged and the discontinuity moves away from the model axis.

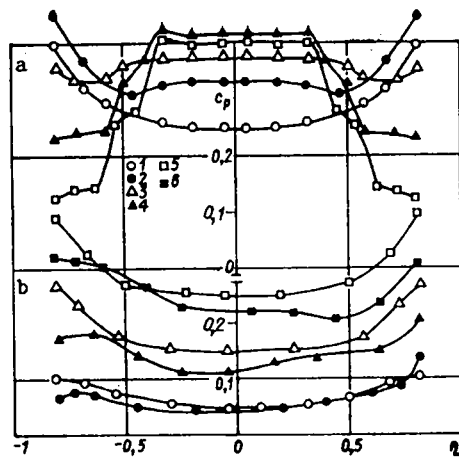


Fig. 2

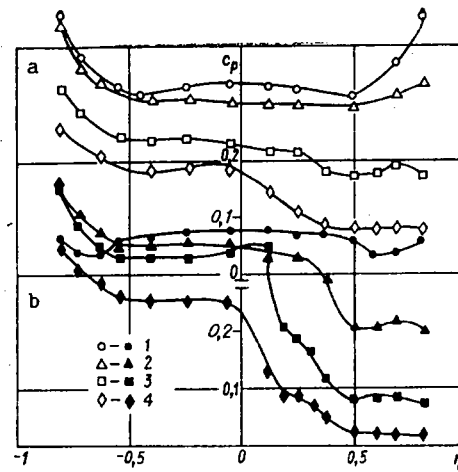


Fig. 3

The field of total pressure in the plane of symmetry of the wings corresponds to the flow which has passed through one shock, while the pressure distribution along the span of the delta wing is a curve consisting of two or three sections of constant pressure with sharp transitions which correspond to the reflected shock waves formed inside the delta wing. The secondary shocks reflected from the wall are weak and cannot noticeably alter the pressure.

For large vertex angles of delta wings washed at angles of attack and roll a flow scheme forms with an asymmetrical curved shock located below the plane of the leading edges. As one goes to smaller vertex angles one finds asymmetrical schemes of Mach interaction and then regular interaction of the shock waves. Measurements of the pressure field have shown that as the roll angle increases there is a rearrangement of the shock wave scheme, with the descending side of the shock moving inside the wing, and the ascending side moving outwards. A special feature of large roll angles in this case is the generation of internal secondary shocks from one side of the wing. For $\gamma = 20-40^\circ$ on the ascending side we observe a secondary shock which interacts with the basic shock wave system.

We consider the pressure distribution on the arm of a delta wing in symmetric flow at zero roll angle (Fig. 2, a: $\chi = 60^\circ$; $\alpha = 15^\circ$; $\gamma = 0$; 1-5) $\Lambda = 180, 150, 120, 90, 60^\circ$). The graphs of pressure distribution $c_p = (p_i - p_\infty)/q$ along the span were constructed as a function of $\eta = r/R$, where r is the distance from the line of intersection of the internal surfaces of the wings to the pressure tap point, and R is the distance from the tap points to the leading edge. The data illustrate the rearrangement of the flow as the delta angle changes. The distribution of the pressure coefficient over the span is symmetric relative to the central chord, and therefore the graphs (Fig. 2, a) show the left semi-span of the delta wing.

In the case of a planar triangle wing ($\Lambda = 180^\circ$) a curved shock is formed, attached to the leading edges, and the pressure decreases from the leading edge to the mean chord. The deviation of wings at angle $\Lambda = 150^\circ$ leads to an increased pressure in the middle part of the delta wing. The regime with a planar shock attached to the sharp leading edge corresponds to constant pressure over the span. The calculated values of delta angle for a given delta wing ($\chi = 60^\circ$) with a planar shock at the leading edges at $M = 3$ are, for $\alpha = 5^\circ$, $\Lambda = 111.5^\circ$; $\alpha = 10^\circ$, $\Lambda = 113.8^\circ$; $\alpha = 15^\circ$, $\Lambda = 114.9^\circ$. For vertex angles less than the calculated value there is a qualitative rearrangement of the flow, where the pressure increases over the span at a certain section. This type of pressure distribution curve is typical for flow with a system of waves falling within the delta wing, when a Mach wave interaction is found. A successive decrease of the vertex angle leads to regular interaction of the shock waves, with several pressure steps, as is observed for $\Lambda = 60^\circ$.

The shape of the pressure distribution curve is different for variation of Λ as a function of the structure of the wave system; the equilibrium pressure distribution is replaced by a stepwise distribution with a sharp or smooth pressure increase. The pressure increase on the wing wall is associated with interaction of the shocks with the boundary layer. In

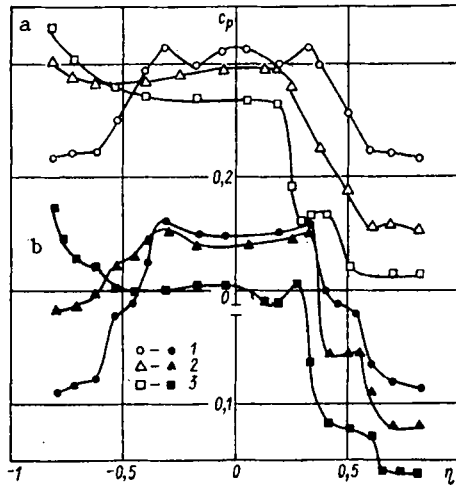


Fig. 4

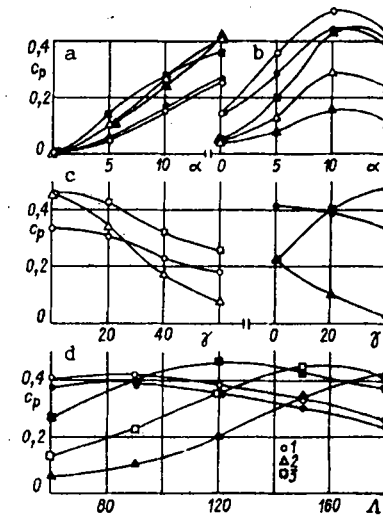


Fig. 5

all the tests a decrease of the vertex angle contracts the section of minimum pressure near the leading edge.

We now consider the pressure distribution on delta wings at roll angles given for specific angles of attack. In contrast with the symmetric flow the assignment of the delta wing roll angle varies the orientation of the left and right surfaces of the delta wing relative to the incident velocity vector. For the counter-flow type of model the roll angle is given by the clock position, and the right wing (descending) corresponds to positive values, while the left wing (ascending) corresponds to negative values. In Fig. 2, b ($\Lambda = 180^\circ$; $\gamma = 0$ open symbols, $\gamma = 40^\circ$ closed symbols; 1, 2) $\alpha = 5^\circ$; 3, 4) $\alpha = 10^\circ$; 5, 6) $\alpha = 15^\circ$) we show the test data for a planar triangular wing. While for $\alpha = 5^\circ$ large roll angles (up to $\gamma = 40^\circ$) do not produce appreciable change of the symmetric pressure distribution, for $\gamma = 40^\circ$ the pressure decreases on both the right half of the delta wing, and on the left half near the leading edges.

The flow over a delta wing with angle $\Lambda = 150^\circ$ for various roll angles is shown in Fig. 3, a ($\Lambda = 150^\circ$; $\alpha = 15^\circ$; 1-4) $\gamma = 0, 20, 40, 60^\circ$). The difference from the planar wing is that the flow with roll angle leads to a reduced pressure on the right half of the delta wing, and not on the left half. Since the aim of these investigations is not only to obtain data for a delta wing at real angles of attack and roll, but also to study asymmetric flow over an angular configuration with a conical stream, in the experiments we investigated large roll angles (up to $\gamma = 60^\circ$). As can be seen, at large angles of attack and roll the pressure decreases sharply both on the right half and on the left half of the delta wing, with the more noticeable decrease on the right half.

If in the previous case with a curved attached shock the pressure is reduced on both sides, then for $\Lambda = 120^\circ$ (Fig. 3, b: $\Lambda = 120^\circ$; $\alpha = 15^\circ$; 1-4) $\gamma = 0, 20, 40, 60^\circ$) at roll angles of 20° and 40° on the right side and in the central section of the left side it is also reduced, forming on the right side a stepwise pressure distribution corresponding to Mach shock interaction. However, on the left side, beginning with $\eta = 0.6$, the pressure for $\gamma = 20$ and 40° increases and exceeds the level for the symmetric flow. With decrease of the angle Λ the shape of the pressure distribution curves changes qualitatively for the two constant pressure sections adjacent to the leading edge, and a stepwise distribution is formed, corresponding to regular shock interaction. In this case the flow asymmetry still appreciably affects the pressure distribution both on the left and on the right half of the delta wing.

3. Star-Shaped Body. The delta wing configuration with angle $\Lambda = 90^\circ$ can be regarded as an element of a star-shaped body with four petals. It should be noted that at present quite detailed studies have been done of flow in the corners [9-11], and most of the papers deal with interaction of the streams inside the right angle [10]. As a rule, angles have been studied with leading edges normal to the incident flow direction [9], but cases with sweptback leading edges have also been considered. [11].

For the model investigated, an element of a four-pointed star with $\Lambda = 90^\circ$ (Fig. 4, a: $\chi = 60^\circ$; $\Lambda = 90^\circ$; $\alpha = 15^\circ$; 1-3) $\gamma = 0, 20, 40^\circ$) the transition from $\gamma = 0$ to $\gamma = 20$ and 40° for all values of angle of attack leads to a decrease of pressure on the descending half and an increase on the ascending half, and for $\alpha = 15^\circ$ on the greater part of the ascending wing the pressure varies very little, and only near the edge is a further increase observed. As one would expect, an asymmetrical system is formed of interacting shock waves with stronger shocks on the ascending side of the wing. On the descending wing the shape of the curve is maintained, with two constant pressure parts, and the ascending section of increased pressure occupies the entire half span of the wing, and there is a tendency towards a stronger pressure increase in the direction to the leading edge, compared to the section of increased pressure in the plane of symmetry of the model. All of this indicates that the configuration with Mach shock interaction inside the delta-shaped wing is rearranged asymmetrically.

For an element of a six-pointed star (Fig. 4, b: $\chi = 60^\circ$; $\Lambda = 60^\circ$; $\alpha = 15^\circ$; 1-3) $\gamma = 0, 20, 40^\circ$) the pressure distribution for $\gamma = 0$ takes the form of three levels of almost constant pressure, and setting the model at roll angles maintains this kind of distribution for all values only on the descending side and for $\gamma = 20^\circ$ on the ascending side. For $\gamma = 40^\circ$ the descending inside half of the delta wing becomes windward, since the angle $\gamma = 40^\circ$ exceeds the half angle of this element and partially covers the ascending half. It is interesting that in this case on the ascending half a similar stepwise pressure distribution is retained. For $\gamma = 40^\circ$ we find an expansion of the flow in the shaded region near the edge in the descending half (in the Prandtl—Meier wave), with supersonic speed maintained near the shaded surface of the wing. This is confirmed by a sharp pressure decrease, where c_p becomes negative. The shock from the descending wing arm interacts with the boundary layer on the ascending part of the wing. However, the angle between the incident flow velocity vector and the ascending arm increases, which leads to increased pressure near the wing edge.

Figure 5 shows the dependence of pressure on the models of wings and star-shaped bodies as a function of the angle of attack. To analyze the relations $c_p = f(\gamma)$ we chose characteristic points over the wing spans: on the line of meeting of the two halves of the delta wing $\eta = 0$ and near the leading edges $\eta = 0.8$ and -0.8 . As one would expect, for the model of a planar triangular wing the pressure increases with increase of the angle of attack (Fig. 5, a: $\Lambda = 180^\circ$; $M = 3$; $\gamma = 0$ open symbols, $\gamma = 20^\circ$ closed symbols; 1-3) $\eta = 0, 0.81, -0.81$). Also, for the model of an element of a four-pointed star the maximum pressure is found at $\alpha = 10^\circ$, which is associated with a change of the shock wave configuration (Fig. 5, b: $\Lambda = 90^\circ$; $M = 3$; $\gamma = 0$ open symbols, $\gamma = 20^\circ$ closed symbols; 1-3) $\eta = 0; 0.81, -0.81$). In the investigations of flow over elements of star-shaped bodies in [12] it was noted also that the maximum pressure was obtained near $\alpha = 10^\circ$. This is explained by transition from regular shock wave interaction to Mach interaction.

We now consider the influence of γ on the pressure variation over the span of delta wings. The values of the angles $\Lambda = 150$ and 90° correspond to the waverider and four-pointed configurations. Figure 5, c shows the pressure coefficients for $M = 3$ and $\alpha = 15^\circ$ ($\Lambda = 150^\circ$ for the open symbols, $\Lambda = 90^\circ$ closed symbols; 1-3) $\eta = 0, 0.81, -0.81$). For $\Lambda = 150^\circ$ an increase of roll angle causes a decrease of pressure on all the wing surfaces, and near the leading edge of the descending wing it decreases more than on the centerline ($\eta = 0$). In contrast with $\Lambda = 150^\circ$ for the star element with $\Lambda = 90^\circ$ the pressure on the ascending arm ($\eta = -0.8$) increases, and on the centerline and on the descending arm it also decreases.

There is interest in studying flow over delta wings at roll angles over the entire range of vertex angle. As in the previous case, we constructed the pressures at the three characteristic points (Fig. 5, d: $M = 3$; $\alpha = 15^\circ$; $\gamma = 0$ open symbols, $\gamma = 20^\circ$ closed symbols; 1-3) $\eta = 0, 0.81, -0.81$). For flow over delta wings at zero roll angle the maximum pressure near the leading edges is obtained for $\Lambda = 150^\circ$, and on the centerline at $\Lambda = 90^\circ$. The transition to $\gamma = 20^\circ$ gives a maximum pressure on the ascending arm for $\Lambda = 120^\circ$, and on the descending arm for $\Lambda = 180^\circ$. We note that setting $\gamma = 40^\circ$ leads to transition of the maximum pressure on the ascending arm to $\Lambda = 90^\circ$.

LITERATURE CITED

1. T. R. F. Nonweiler, Aerodynamic problems of manned space vehicles, " J. R. Aeron. Soc., 63, 521 (1959).
2. A. L. Gonor and A. I. Shvets, "Supersonic flow over V-shaped wings at $M = 3.9$," Izv. Akad. Nauk SSSR, Mekh. Zhidk. Gaza, No. 6 (1967).

3. Yu. P. Gun'ko and I. I. Mazhul', "Flow over the lower surface of V-shaped wings at Mach numbers less than design," *Izv. Sib. Otdel. Akad. Nauk SSSR, Ser. Tekhn. Nauk*, No. 3, Issue 1 (1977).
4. G. I. Maikapar, "The wave drag of non-axisymmetric bodies at supersonic speeds," *Zh. Prikl. Mekh. Matem.*, 23, No. 2 (1959).
5. M. N. Kazakov, V. V. Kravets, and A. I. Shvets, "Aerodynamic coefficients of non-conical bodies with star-shaped cross sections," *Izv. Akad. Nauk SSSR, Mekh. Zhidk. Gaza*, No. 6 (1974).
6. Yu. A. Vedernikov, V. G. Dulov, and A. F. Latypov, "Optimization of hypersonic three-dimensional bodies," *Zh. Prikl. Mat. Teor. Fiz.*, No. 1 (1979).
7. J. Venn and J. Flower, "Shock patterns for simple caret wings," *Aeronaut. J.*, 74, 339 (1970).
8. J. Kipke, Untersuchungen an schiebenden Wellenreiter-Flugeln im Hyperschallbereich, *Z. Flugwiss.*, 21, No. 11 (1973).
9. A. Charout and L. Redekeopp, "Supersonic flow in the corner formed by two intersecting wedges," *Raket. Tekh. Kosmon.*, No. 3 (1967).
10. P. Kutler, "Supersonic flow in a corner formed by two wedges," *Raket. Tekh. Kosmon.*, No. 5 (1974).
11. V. S. Dem'yanenko and V. P. Fedosov, "Supersonic flow around a concave two-panel corner," *Izv. Sib. Otd. Akad. Nauk SSSR, Ser. Tekhn. Nauk*, No. 13, Issue 3 (1975).
12. A. L. Gonor and A. I. Shvets, "Investigation of the pressure distribution on star-shaped bodies," *Zh. Prikl. Teor. Fiz.*, No. 6 (1965).